International Journal of Bifurcation and Chaos, Vol. 20, No. 5 (2010) 1527–1532

DOI: 10.1142/S0218127410026678

# LOWEST STABILITY BOUNDARY ON FLOW OF CONCENTRIC ROTATING CYLINDERS

H. C. LIN* and W. M. YANG†
*Department of Mechanical Engineering,*
*National Chiao Tung University,*
*1001 Ta Hsueh Road, Hsinchu 300, Taiwan 30010, R.O.C.*
**herojake.lin@gmail.com*
†*wmyang@cc.nctu.edu.tw*

Received June 5, 2009; Revised August 7, 2009

In this study, we numerically investigate the lowest instability boundary of nonaxisymmetric Taylor vortex flow (TVF) for different axial wavenumbers. The variation in the axial wavenumber of a supercritical TVF can affect the instability of the flow, because the wavelength of a Taylor vortex is constant only when the flow is axisymmetrical. When the nonaxisymmetric TVF is transformed to a wavy vortex flow (WVF), the instability boundary is changed with the variation in the axial wavenumber. We carry out an instability analysis of the nonaxisymmetric TVF between two concentric rotating cylinders, which have a radius ratio of 0.88.

*Keywords*: Instability; Taylor vortex; wavy vortex; Taylor–Couette flow; Chebyshev method.



## 1. Introduction

After the Taylor vortex flow (TVF) problem had teetered on the brink of being classified as a nonlinear problem for many years, Coles [1965] was the first to report on the nonuniqueness of the wavy vortex flow (WVF) in the Taylor–Couette flow. The entire pattern of wavy vortices moves with a uniform velocity in the azimuthal direction. Since the term "wavy" is typically associated with motion that includes periodic vertical oscillations, this study emphasizes that WVF move in the azimuthal direction as rings that have $k_1$ fixed sinusoidal upward and downward deformations, where $k_1$ is an integer number of azimuthal waves. WVF was observed by Taylor [1923], Lewis [1928], Coles [1965], and Schultz-Grunow and Hein [1956]; however, they were not recognized as a characteristic feature of the flow. After Coles' preliminary results were published, WVF was also observed by Nissan *et al.* [1963]. Schwarz *et al.* [1956] conducted experiments in which a nonaxisymmetric mode with azimuthal wavenumber $k_1 = 1$ was observed.

Burkhalter and Koschmieder [1929] found that in the case of large radius ratios, the wavelength of axisymmetrical vortices is independent of the Reynolds number in fluid columns of infinite length; the Reynolds number in such fluid columns increases quasi-statically. However, the wavelength of Taylor vortices is constant only as long as the flow is axisymmetrical. Jones [1985] presented the instability boundary for an axial wavenumber of 3.13, the critical value for a quasi-static transition, for a wide range of radius ratios. Jones [1985] considered the problem of calculation of nonlinear axisymmetrical Taylor vortices. A spectral method together with Newton–Raphson iterations was used to solve the nonlinear algebraic equations.

While Taylor's study analyzed Tayor–Couette flow under supercritical conditions, Stuart [1958] observed that the shape, i.e. the size, of the vortices remains unchanged above the critical Reynolds number. Numerous studies (see [Ahlers *et al.*, 1982; Andereck *et al.*, 1986; Coles, 1965; Park *et al.*, 1981; Burkhalter & Koschmieder, 1929, 1973; Antonijoan, 2002]) have demonstrated the importance of

considering the acceleration/deceleration of the flow in determining the final state of the flow. These vortices have axial wavelengths that are different from those of vortices observed after a quasi-static transition. The present study demonstrates that the instability boundary occurs at a critical wavelength corresponding to the quasi-static transition in addition to another wavelength. These solutions are related to the standard Taylor vortices and can be obtained quasi-statically for certain radius ratios when a mechanism is used for modifying the axial wavelength (see [Hall, 1979]).



## 2. Numerical Method

The system geometry is specified by the inner radius $R_1$ and outer radius $R_2$ of the cylinders with an infinite aspect ratio. $R_i = R_1\Omega_1 d/\nu$ and $R_o = R_2\Omega_2 d/\nu$ are the Reynolds numbers in the case of the inner and outer cylinder rotations, $\nu$ is the dynamic viscosity, $\Omega_1$ and $\Omega_2$ are the angular velocity of the inner and outer cylinder rotations and $d = R_2 - R_1$ is the gap of the cylinders, respectively. The dimensionless parameters in this problem are the radius ratio $\eta = R_1/R_2$, axial wavenumber $\alpha$, and axial wavelength $\lambda(\lambda = 2\pi/\alpha)$ (see Table 1). First, the TVF is solved numerically. The solutions to the Navier–Stokes equations are determined using a pseudo-spectral Fourier–Chebyshev collocation method, taking advantage of the orthogonality properties of Chebyshev polynomials and assuming exponential convergence. The space can be defined as $T_n(\xi) = \cos(n \cdot \cos^{-1}\xi)$, and $\phi_n$ is a base function that satisfies the boundary conditions. $\phi_n$ is expressed as

$$\phi_n(\xi) = T_n - [1 - (-1)^n]\frac{T_1}{2} - [1 + (-1)^n]\frac{T_0}{2}, \quad n = 2, 3, 4, \ldots \tag{1}$$

where $\xi \in [-1, 1]$. The domain of $r$ in the governing equation is transformed from $\eta/(1-\eta) \le r \le 1/(1-\eta)$ to $-1 \le \xi \le 1$ through the relational equation $\xi = 2r - (1+\eta)/(1-\eta)$. The time scheme is semi-implicit and second-order accurate. It corresponds to a combination of the second-order backward implicit Euler scheme (for the time term) and an explicit Adam–Bashforth scheme (for the nonlinear terms). The discretized form of the momentum equation is

$$\frac{3\mathbf{V}^{j+1} - 4\mathbf{V}^{j} + \mathbf{V}^{j-1}}{2\delta t} + 2(\mathbf{V}^{j} \cdot \nabla)\mathbf{V}^{j} - (\mathbf{V}^{j-1} \cdot \nabla)\mathbf{V}^{j-1} = -\nabla p^{j+1} + \frac{1}{R_e}\Delta \mathbf{V}^{j+1} \tag{2}$$

where $\mathbf{V} = (\overline{V}_r, \overline{V}_\theta, \overline{V}_z)$ and $j$ is the solution at time $t_j = j\delta t$, $\delta t$ being the time step. We assume infinite cylinders with fix rotational speed and a periodic solution in the axial direction. The boundary conditions are

$$\overline{V}_r = \overline{V}_z = 0, \quad \overline{V}_\theta = R_i \quad \text{at } \xi = -1, \quad \text{and}$$
$$\overline{V}_r = \overline{V}_z = 0, \quad \overline{V}_\theta = R_o \quad \text{at } \xi = 1 \tag{3}$$

The flow velocity and pressure profile of the supercritical TVF are obtained using the following equations:

$$\overline{V}_r = \sum_{m=0}^{M-1}\sum_{n=2}^{N+1} A_{mn}\phi_n(\xi)\cos m\alpha Z \tag{4}$$

$$\overline{V}_\theta = \overline{\overline{V}}(r) + \sum_{m=0}^{M-1}\sum_{n=2}^{N+1} B_{mn}\phi_n(\xi)\cos m\alpha Z \tag{5}$$

$$\overline{V}_z = \sum_{m=1}^{M}\sum_{n=2}^{N+1} C_{mn}\phi_n(\xi)\sin m\alpha Z \tag{6}$$

$$\overline{p} = \sum_{m=0}^{M-1}\sum_{n=0}^{N-1} D_{mn}T_n(\xi)\cos m\alpha Z \tag{7}$$

Here, $M$ and $N$ are the number of terms in the Fourier series expansion and Chebyshev polynomial expansion, respectively, and $A_{mn}, B_{mn}, C_{mn}$ and $D_{mn}$ are amplitude coefficients. $\overline{\overline{V}}(r)$ is the basic flow velocity of one-dimensional Couette flow.

Table 1. Notations.

| Dimensionless Parameters | | | |
|---|---|---|---|
| $R_i$ | Reynolds number of inner cylinder rotation | $\lambda$ | Axial wavelength |
| $R_o$ | Reynolds number of outer cylinder rotation | $T_a$ | Taylor number |
| $\eta$ | Radius ratio | $k_1$ | wavenumber of the perturbation in the azimuthal direction |
| $\alpha$ | Axial wavenumber | $k_2$ | wavenumber of the perturbation in the axial direction |

The momentum and continuity equations are transformed into an algebraic equation, which can be expressed as a matrix equation:

$$\begin{bmatrix} A_{11} & 0 & 0 & A_{14} \\ 0 & A_{22} & 0 & 0 \\ 0 & 0 & A_{33} & A_{34} \\ A_{41} & 0 & A_{43} & 0 \end{bmatrix} \begin{bmatrix} A_{mn} \\ B_{mn} \\ C_{mn} \\ D_{mn} \end{bmatrix}^{i+1} = \begin{bmatrix} F_1 \\ F_2 \\ F_3 \\ 0 \end{bmatrix}^{i,i-1} \quad (8)$$

The matrix equation represents a system of equations with $(4 \times M \times N)^2$ unknown parameters. The coefficients $A_{mn}, B_{mn}, C_{mn}$ and $D_{mn}$ are determined iteratively until the convergence condition is satisfied. When the cylinders rotate with a fixed rotational speed, the convergence condition is

$$\left| \frac{A^i_{mn} - A^{i-1}_{mn}}{A^{i+1}_{mn}} \right| < 10^{-4} \quad (9)$$

The coefficient that satisfies the convergence condition is substituted in the appropriate equation among Eqs. (4)–(7); the speed and pressure in each time interval can then be determined. If the cylinders rotate periodically, the largest value of axial speed attained in a particular time interval at a selected observation point in the flow is compared with the axial speed in the preceding time interval. If the difference is less than $10^{-4}$, then the convergence condition is considered to be fulfilled.

The instabilities of supercritical TVF are studied by introducing disturbances in the nonlinear TVF. This flow type is expressed as follows:

$$f(V_r, V_\theta, V_z, p) = \overline{f}(\overline{V}_r, \overline{V}_\theta, \overline{V}_z, \overline{p}) + f'(V'_r, V'_\theta, V'_z, p') \quad (10)$$

where $\overline{f}$ denotes the flow velocity and pressure profile of the supercritical TVF and $f'$ represents the perturbations. The equations employed for the analysis, only out-of-phase wavy modes are investigated, of perturbations in normal modes are as follows:

$$V'_r = \sum_{q=1}^{Q} \sum_{s=2}^{S+1} a_{qs} \phi_s(\xi) \sin q\alpha Z \cdot \exp[\sigma\tau + i(k_1\theta + k_2 Z)] \quad (11)$$

$$V'_\theta = \sum_{q=1}^{Q} \sum_{s=2}^{S+1} b_{qs} \phi_s(\xi) \sin q\alpha Z \cdot \exp[\sigma\tau + i(k_1\theta + k_2 Z)] \quad (12)$$

$$V'_Z = \sum_{q=0}^{Q-1} \sum_{s=2}^{S+1} c_{qs} \phi_s(\xi) \cos q\alpha Z \cdot \exp[\sigma\tau + i(k_1\theta + k_2 Z)] \quad (13)$$

$$p' = \sum_{q=1}^{Q} \sum_{s=0}^{S-1} d_{qs} T_s(\xi) \sin q\alpha Z \cdot \exp[\sigma\tau + i(k_1\theta + k_2 Z)] \quad (14)$$

Here, $Q$ and $S$ are the number of terms in the Fourier series expansion and Chebyshev polynomial expansion, respectively. $k_1$ (an integer) and $k_2$ (a real number) are wavenumbers of the perturbations in the azimuthal and axial directions, respectively, and $a_{qs}, b_{qs}, c_{qs}$ and $d_{qs}$ are amplitude coefficients.

The dimensionless Navier–Stokes and continuity equations are as follows:

$$\partial_t \mathbf{f} + \mathbf{f} \cdot \nabla \mathbf{f} = -\nabla p + \Delta \mathbf{f}, \quad \nabla \cdot \mathbf{f} = 0 \quad (15)$$

The boundary conditions are

$$f' = 0 \quad \text{at } \xi = -1 \quad \text{and} \quad \xi = 1 \quad (16)$$

Substituting Eq. (10) into Eq. (15) and linearizing the dimensionless Navier–Stokes equation, we can obtain the characteristic perturbation equations, which constitute a generalized eigenvalue problem:

$$AX = \sigma BX, \quad A = \begin{bmatrix} A_{11} & A_{12} & A_{13} & A_{14} \\ A_{21} & A_{22} & A_{23} & A_{24} \\ A_{31} & 0 & A_{33} & A_{34} \\ A_{41} & A_{42} & A_{43} & 0 \end{bmatrix},$$

$$B = \begin{bmatrix} B_{11} & 0 & 0 & 0 \\ 0 & B_{22} & 0 & 0 \\ 0 & 0 & B_{33} & 0 \\ 0 & 0 & 0 & 0 \end{bmatrix}, \quad (17)$$

$$X = \begin{bmatrix} a_{qs} \\ b_{qs} \\ c_{qs} \\ d_{qs} \end{bmatrix}$$

Here, $A$ and $B$ are complex matrices that depend on $k_1$ and $k_2$, and the eigenvector $X$ contains the amplitudes of the eigenfunctions. The stability of the flow can be determined by the real part of the growth rate of a complex disturbance $\sigma$. When $\sigma_r < 0$, the entire flow is stable. The disturbance decreases with an increase in time. When $\sigma_r > 0$, the disturbance increases with time and the

flow becomes unstable. When $\sigma_r = 0$, the flow has neutral stability.

The eigenvalue of the generalized eigensystem is obtained by using the subroutine DGVLCG in the IMSL library, which determines all eigenvalues with a high level of accuracy. $R_i$ is searched on the neutral stable curve, i.e. the curve on which the real part of the most unstable eigenvalue vanishes, using the secant method; this method requires two initial guesses. The iteration is not terminated until the real part of the most unstable eigenvalue is less than $10^{-6}$. The $R_i$ values for different axial wavenumbers can be obtained for neutral stable states. The minimum Reynolds number is called the critical Reynolds number and corresponds to the critical axial wavenumber.

## 3. Results and Discussion

Theoretically, the greater the number of terms in the Fourier series expansion and Chebyshev polynomial expansion, the higher is the accuracy of the eigenvalues determined; however, the use of too many terms will render the computation time-consuming. Therefore, the best option is to consider the least number of terms in the expansion that can provide the required accuracy. A comparison was made between the values obtained from the $M$ and $N$ terms in the computational model of the TVF used in this study and the values obtained by Jones [1985] for the case where the inner cylinder rotated at a constant velocity and outer cylinder is stationary. Jones [1985] used the Taylor number to obtain the rotational velocity of the inner cylinder; the velocities obtained by Jones [1985] are listed in Table 2.

When a low $R_i$ ($R_i = 72.5$) is derived, both $M$ and $N$ are increased to 6 terms and each velocity component of the flow field converges to 0.19%. However, when a high $R_i$ ($R_i = 259.8$) is derived, both $M$ and $N$ are increased to more than 10 so that each velocity component of the flow field can converge to 0.14%. These results are in agreement with those obtained by Jones [1985]. As shown in Table 2, in this study, the number of terms considered for the computation of the eigenvalues of the TVF $(M, N)$ and WVF $(Q, S)$ is ten.

Figure 1 shows the numerical result (with $k_2 = 0$) together with the experimental data obtained by Ahlers *et al.* [1982]. Each symbol (solid circle) corresponds to a solution in their study (onset of the WVF at $k_1 = 3$). The range of axial wavenumbers considered is 2.6–4.0 and the range of $R_i/R_{i,c}$ is 0.8–2.0. $R_{i,c}$ is the critical value of $R_i$, i.e. the value at which the axisymmetrical TVF occurs. The model used in the present study assumes that the WVF are perfectly periodic in the axial direction and thus ignores the end effects. This model is similar to that developed by Ahlers *et al.* [1982]. A comparison of the model used in the present study with the models developed by Park [1984] and Jones [1981] indicates that the agreement between experimental and theoretical values for $k_1 = 2$ is good. $k_1 = 3$ is out of the scope of Jones [1981] and this study (see Table 3).

The regime diagram of the onset of WVF was determined by Coles [1965]. The Coles' result is a

Table 2. When the outer cylinder is stationary and the inner cylinder is revolving at a constant velocity, the radial velocity at the observatory point is $\eta = 0.5$ $(\xi = 0, \mathrm{Z} = 0)$ $(T_a = 2(1-\eta)R_i^2/(1+\eta))$.

| $R_i$ / $T_a$ / $M \times N$ | 72.5 (3500) | 106.1 (7500) | 150 (15000) | 212.1 (30000) | 259.8 (45000) |
|---|---|---|---|---|---|
| $4 \times 4$ | 4.6991 | 17.5775 | — | — | — |
| $5 \times 5$ | 3.9956 | 17.1988 | 30.5700 | 41.92323 | — |
| $6 \times 6$ | 4.2333 | 17.8566 | 32.8350 | 52.7493 | 67.0024 |
| $7 \times 7$ | 4.2253 | 17.9733 | 33.5851 | 52.8491 | 69.8342 |
| $8 \times 8$ | 4.2340 | 17.9840 | 33.5712 | 54.9975 | 70.7955 |
| $9 \times 9$ | 4.2376 | 17.9733 | 33.6452 | 55.5914 | 71.8347 |
| $10 \times 10$ | 4.2354 | 17.9840 | 33.6900 | 55.6550 | 72.2764 |
| $11 \times 11$ | 4.2347 | 17.9840 | 33.6754 | 55.6763 | 72.3803 |
| $12 \times 12$ | 4.2354 | 17.9840 | 33.6754 | 55.6975 | 72.4063 |
| $13 \times 13$ | 4.2354 | 17.9840 | 33.6754 | 55.6975 | 72.4063 |
| Study of Jones [1985] | 4.2336 | 17.9733 | 33.6768 | 55.7187 | 72.2764 |

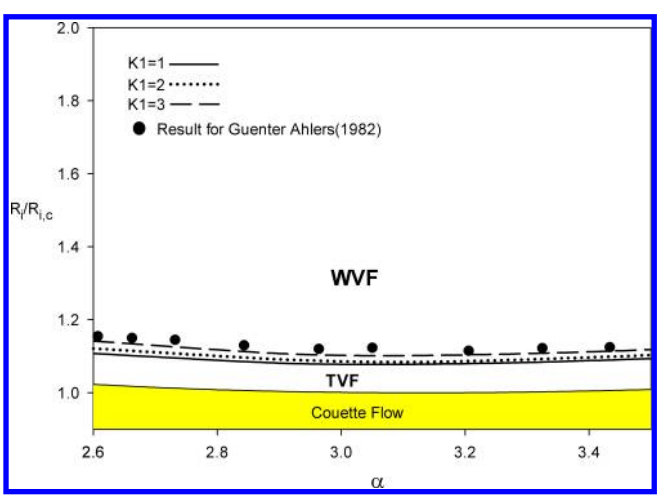


Fig. 1. Experimental curves for the onset of WVF for $\eta = 0.893$.

Table 3. Comparison of experimental and theoretical values for $\eta = 0.782$.

| | | Numerical Method | |
|---|---|---|---|
| | Experiment (Park [1984]) | Study of Jones [1981] | This Study |
| Onset of $k_1 = 1$ | Not observed | 110 | 109.5 |
| Onset of $k_1 = 2$ | 137.3 | 120 | 119.5 |
| $k_1 = 2$ gone | 161.3 | 163 | 167.5 |
| $k_1 = 1$ gone | Not observed | 169 | 167.8 |
| Onset of $k_1 = 3$ | 322 | None | None |



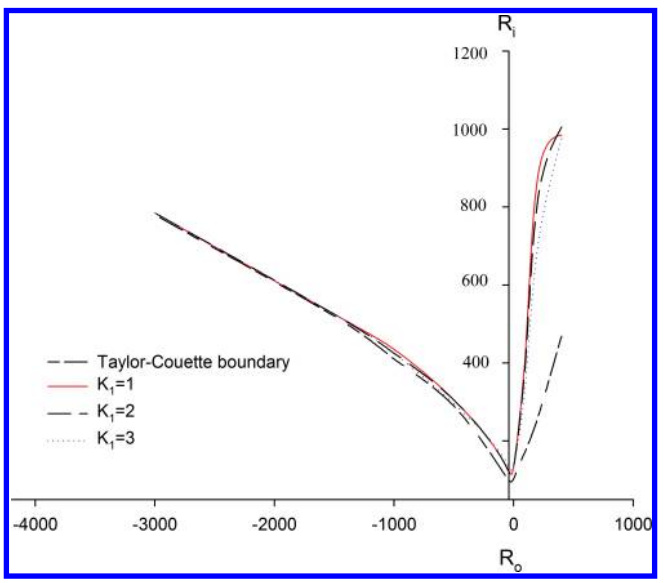


(a)

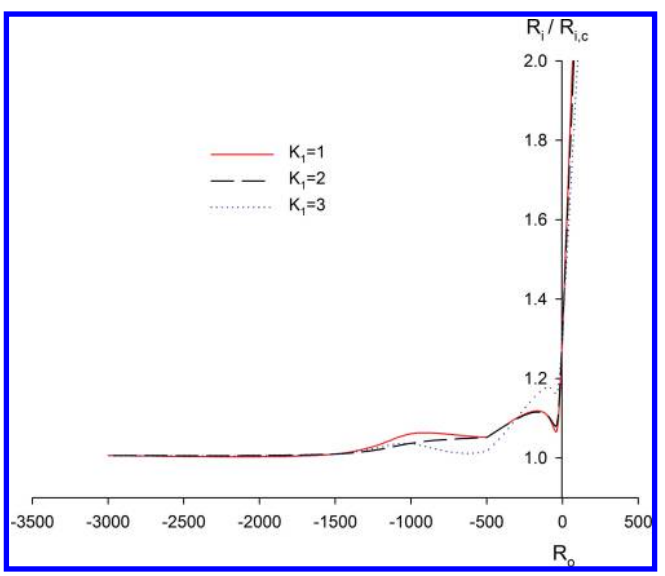


(b)

Fig. 2. Lowest stability boundary for different azimuthal wavenumbers $k_1$ corresponding to nonaxisymmetric TVF that is transformed to a WVF (a) for $R_i$ versus $R_o$ (b) for $R_i/R_{i,c}$ versus $R_o$.

remarkable confirmation of Taylor's [1923] stability diagram for the onset of axisymmetric TVF as a function of the rotation rate of both cylinders. The nonaxisymmetric TVF will be transformed to WVF when the rotational speed of the cylinders exceeds the critical value $R_{i,c}$, the instability boundary will be changed with different axial wavelength, rotational direction and speed of the cylinders. In this study, we consider the case wherein $\eta = 0.88, \alpha = 2.7$–$3.5$, and $k_1 = 1$–$3$, and we solve the lowest instability boundary of TVF for two concentric rotating cylinders. Figure 2(a) shows that the TVF is more stable during corotation rather than counterrotation of the cylinders. In the case of flow in corotational cylinders, the lowest instability occurs when $R_i/R_{i,c} = 2$–$4$ for $0 < R_o < 400$; however, $R_i/R_{i,c} = 1.31$ for $R_o = 0$. The numerical result is in good agreement with that obtained by Coles [1965]. However, with regard to the flow in the case of counterrotating cylinders, the instability boundary, with various azimuthal wavenumbers $k_1 = 1$–$3$ and axial wave numbers $\alpha = 2.7$–$3.5$, is different from that of axisymmetric TVF. Figure 2(b) shows that the lowest TVF instability boundary occurs when the rotational speed of the outer cylinder is (1) $-290 \leq R_o \leq 0$ for $k_1 = 1$ or 2, (2) $-1000 \leq R_o \leq -290$ for $k_1 = 3$, and (3) $-1300 \leq R_o \leq -1000$ for $k_1 = 2$ or 3. When $R_o(-4000 \leq R_o \leq -1300)$ increases gradually for any value of $k_1$, the instability of TVF is occurrs immediately by $R_i/R_{i,c} = 1.006-1.06$.

## 4. Conclusion

We investigated the lowest stability boundary in the case of different azimuthal wavenumbers $k_1$ corresponding to a nonaxisymmetric TVF that is transformed to a WVF. The effect of the variation of the axial wavenumber of a TVF on the instability of the flow can be studied by using an infinite cylinder approximation. The axial wavenumber is considered

as an external parameter and is not determined theoretically, but is measured experimentally. In some apparatuses, such as those used by King and Swinney [1982], fluid can be added or removed even during the rotation of the cylinders, thereby allowing direct control of the axial wavelength. In the present study, we determined a new lowest stability boundary curve for the transition from a supercritical TVF to a WVF. This curve differs from that obtained by Coles [1965], who assumed that the TVF was axisymmetric and that the Reynolds number of the cylinders increased quasi-statically.

## References


Ahlers, G., Cannell, D. S. & Lerma, M. A. D. [1983] "Possible mechanism for transitions in wavy Taylor-vortex flow," *Phys. Rev. A. At. Mol. Opt. Phys.* **27**, 1225–1227.

Andereck, C., Liu, S. S. & Swinney, H. L. [1986] "Flow regimes in a circular Couette system with independently rotating cylinders," *J. Fluid Mech.* **164**, 155–183.

Antonijoan, J. & Sanchez, J. [2002] "On stable Taylor vortices above the transition to wavy vortices," *Phys. Fluids* **14**, 1661–1665.

Burkhalter, J. E. & Koschmieder, E. L. [1973] "Steady supercritical Taylor vortex flow," *J. Fluid Mech.* **58**, 547–560.

Burkhalter, J. E. & Koschmieder, E. L. [1974] "Steady supercritical Taylor vortices after sudden starts," *Phys. Fluids* **17**, 1929–1935.

Coles, D. [1965] "Transition in circular Couette flow," *J. Fluid Mech.* **21**, 385–425.

Hall, P. & Blennerhasset, P. J. [1979] "Centrifugal instability of circumferential flow in finite cylinders," *Proc. R. Soc. London A* **365**, 191–207.

Jones, C. A. [1981] "Nonlinear Taylor vortices and their stability," *J. Fluid Mech.* **102**, 249–261.

Jones, C. A. [1985a] "The transition to wavy Taylor vortices," *J. Fluid Mech.* **157**, 135–162.

Jones, C. A. [1985b] "Numerical method for the transition to wavy Taylor vortices," *J. Comput. Phys.* **61**, 321–344.

King, G. P. & Swinney, H. L. [1983] "Limits of stability and irregular flow patterns in wavy vortex flow," *Phys. Rev. A. At. Mol. Opt. Phys.* **27**, 1240–1243.

Lewis, J. W. [1928] "An experimental study of the motion of a viscous liquid contained between two coaxial cylinders," *Proc. R. Soc. London A* **117**, 388–407.

Nissan, A. H., Nardacci, J. L. & Ho, C. Y. [1963] "The onset of different modes of instability for flow between rotating cylinders," *AIChE J.* **9**, 620–624.

Park, K., Gerald, L. & Donnelly, R. J. [1981] "Determination of transition in Couette flow in finite geometries," *Phys. Rev. Lett.* **47**, 1448–1450.

Park, K. [1984] "Unusual transition sequence in Taylor wavy vortex flow," *Phys. Rev. A. At. Mol. Opt. Phys.* **29**, 3458–3460.

Schultz-Grunow, F. & Hein, H. [1956] "Beitrag zur Couettestromung," *Z Flugwiss* **4**, 28–30.

Stuart, J. T. [1958] "On the nonlinear mechanics of hydrodynamic stability," *J. Fluid Mech.* **4**, 1–21.

Taylor, G. I. [1923] "Stability of a viscous liquid contained between two rotating cylinders," *Phil. Trans. R. Soc. London A* **223**, 289–343.